

Model of Convective Taylor Columns in Rotating Rayleigh-Bénard Convection

Ian Grooms,¹ Keith Julien,¹ Jeffrey B. Weiss,² and Edgar Knobloch³

¹*Department of Applied Mathematics, University of Colorado, Boulder, Colorado 80309, USA*

²*Department of Atmospheric and Oceanic Sciences, University of Colorado, Boulder, Colorado 80309, USA*

³*Department of Physics, University of California, Berkeley, California 94720, USA*

(Received 15 February 2010; published 1 June 2010)

Observations, and laboratory and numerical studies, of fluid flows with strong rotation and thermal forcing often show long-lived convective Taylor columns (CTCs) which carry a large portion of the vertical heat and mass fluxes. However, owing to experimental and numerical challenges, these structures remain poorly understood. Here we present a nonlinear, analytical multiscale model of CTCs in the context of rotating Rayleigh-Bénard convection that successfully matches numerical simulations and provides a new multiscale interpretation of the Taylor-Proudman constraint.

DOI: [10.1103/PhysRevLett.104.224501](https://doi.org/10.1103/PhysRevLett.104.224501)

PACS numbers: 47.55.pb, 47.32.Ef, 47.27.De, 47.27.te

Many geophysical and astrophysical phenomena involve fluids under the combined influence of rotation and thermal forcing. Examples include the Sun and stars [1], giant planets [2], and Earth's oceans [3]. As is common in rotating fluids, these phenomena display self-organization into coherent features which dominate the flow. Simple models of coherent features in other complex fluids have led to major advances in understanding and modeling [4–6]. In this Letter, we present a new, analytical, multiscale model of coherent convective columns which successfully describes the structures seen in laboratory experiments [7–9] and quantified in numerical simulations [10–12]. Furthermore, the multiscale nature of the approach provides new insight into the role of the Taylor-Proudman (TP) constraint, improving on previous single-scale interpretations.

The essence of rotating, thermally forced flow is captured by rotating Rayleigh-Bénard convection, i.e., convection in a layer of Boussinesq fluid confined between flat, horizontal, rigidly rotating upper and lower boundaries held at fixed temperatures, with the temperature of the lower boundary higher than that of the upper boundary by an amount $\Delta T > 0$. In this framework, the controlling nondimensional parameters are the (convective) Rossby number (Ro), which measures the strength of rotation relative to thermal forcing, and the Rayleigh number $Ra \propto \Delta T$, which measures the strength of the thermal forcing.

Rotating Rayleigh-Bénard convection has been extensively studied using linear [13], weakly nonlinear [14], and fully nonlinear approaches [15], in addition to numerical [10,11,16] and laboratory [7–9] experiments. These studies attest to the simple fact that the flow tends to self-organize into regions of upwelling hot and downwelling cold fluid, whether the flow is turbulent, as in the case of highly supercritical plume-dominated convection [17], or laminar, as in the case of planform convection [13,18]. In each case, the flow must somehow accommodate the TP constraint. This constraint, formulated theoretically by Taylor [19] following earlier experiments by Proudman [20], explains

why rapid rotation tends to inhibit flow variation along the axis of rotation. For high enough Rayleigh numbers the TP effect is overwhelmed by thermal forcing, while for strong enough rotation the constraint completely inhibits vertical variation of the flow. Between these extremes the competing influences of thermal forcing and rotational (Ekman) friction have a profound effect on the morphology of the flow structures, and for certain parameter regimes long-lived columnar convective structures are observed to form [7–9]. In a recent paper, Portegies *et al.* [21] presented a linear model of these structures. In this Letter we construct a self-consistent *nonlinear* model that agrees well with recent numerical simulations [11,12]. Hereafter we call these structures “convective Taylor columns” (CTCs).

The TP constraint requires that, away from the confining boundaries, the CTCs are nearly uniform vertically. The columns must, however, overcome the TP constraint near the boundaries where the vertically moving fluid slows down, resulting in a strong vertical variation in velocity. It is commonly believed that the required deceleration at the boundaries is accomplished by Ekman boundary layers, i.e., viscous boundary layers influenced by rotation (e.g., [22]). While it is certainly true that Ekman layers can in theory cause strong vertical variations, recent simulations [12] support a different explanation.

The essential morphology of CTCs is that they are tall and thin. This suggests an approach with horizontal scales that are much smaller than the dominant vertical scale. Recent work [23] shows that this scale separation arises naturally in the low Rossby number (rapid rotation) regime. In this regime the Ekman layers are passive [18], but the flow nonetheless organizes into CTCs. Recent simulations [12,21] show that the CTCs in this regime are shielded by a sheath of opposite vorticity and hence interact only weakly. The presence of this shield appears to be a characteristic property of the CTCs in the rapid rotation limit; Fig. 1 shows that this shield is visible in the temperature field as well. Owing to the multiscale nature of the flow, the TP constraint requires vertical variations to be

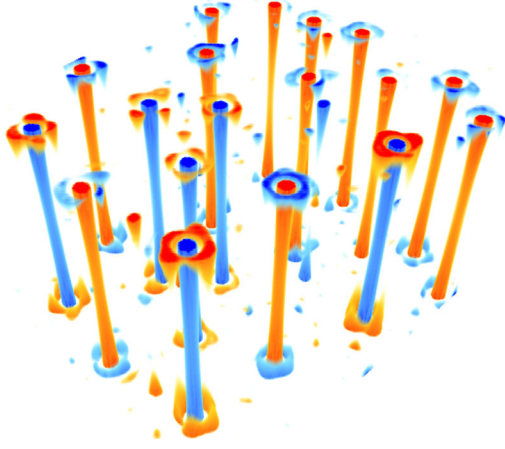


FIG. 1 (color online). A snapshot of the temperature fluctuation θ in the low Rossby number regime. Hot and cold convective Taylor columns span the entire depth of the layer but are shielded by a sheath in which θ takes the opposite sign. Although not visible in the figure, this shield extends throughout the depth. From Ref. [12] with parameters $\tilde{\text{Ra}} = 40$, $\sigma = 7$, visualized as in Ref. [27].

small only on a vertical scale equal to the small horizontal scale of the column width. As a result, on the vertical scale of the entire column, vertical variations can be quite significant, as observed in [12,16], with no need for boundary layers to provide the necessary deceleration.

Our analytical model begins with the balanced equations derived in [23], which incorporate the scale anisotropy described above:

$$\partial_t \omega + J[\psi, \omega] - \partial_z \nabla_{\perp}^2 \phi = \nabla_{\perp}^2 \omega, \quad (1)$$

$$\partial_t \nabla_{\perp}^2 \phi + J[\psi, \nabla_{\perp}^2 \phi] + \partial_z \psi = \sigma^{-1} \tilde{\text{Ra}} \theta + \nabla_{\perp}^4 \phi, \quad (2)$$

$$\partial_t \theta + J[\psi, \theta] + \nabla_{\perp}^2 \phi \partial_z \bar{T} = \sigma^{-1} \nabla_{\perp}^2 \theta, \quad (3)$$

$$\partial_{\tau} \bar{T} + \partial_z (\overline{\theta \nabla_{\perp}^2 \phi}) = \sigma^{-1} \partial_{zz} \bar{T}. \quad (4)$$

These dimensionless equations are written in terms of the horizontal average of the temperature \bar{T} and three “fluctuating” quantities with zero horizontal mean: pressure ψ , vertical velocity w written in terms of the poloidal velocity potential ϕ as $w = \nabla_{\perp}^2 \phi$, and temperature perturbation θ . The vertical component of vorticity is $\omega = \nabla_{\perp}^2 \psi$, and the Jacobian $J[\psi, f] \equiv \partial_x \psi \partial_y f - \partial_y \psi \partial_x f = \mathbf{u}_{\perp} \cdot \nabla f$ represents advection by the horizontal component of velocity indicated by the subscript \perp . The ratio of the horizontal to vertical scales is equal to Ro , and the ratio of the slow time τ to the fast time t is Ro^2 ; the overbar denotes an average over the fast time and horizontal variables (x, y) . The Rayleigh number has been scaled so that $\text{Ra} = \text{Ro}^{-4} \tilde{\text{Ra}}$, with $\tilde{\text{Ra}}$ of order one; σ is the Prandtl number. The equations are obtained via an asymptotic expansion in the Rossby number $\text{Ro} \ll 1$, as appropriate for rapid rotation [12,23]; as a result, Ro no longer appears.

Like the more familiar quasigeostrophic equations, these equations are geostrophically balanced and the leading order horizontal velocity is incompressible. However, unlike the quasigeostrophic equations, these equations incorporate order one vertical motions; this is a consequence of the assumed small horizontal scale of the convective columns. This flow is accompanied by ageostrophic motions which render the flow fully incompressible and by Ekman layers which accommodate no-slip boundaries; both contributions can in principle be calculated *a posteriori* from the solutions of the balanced equations [18,23], but their existence is not felt by and does not change these solutions.

Sprague *et al.* [12] conducted an investigation of the balanced equations using direct numerical simulation (DNS). The authors found that for a wide range of Rayleigh and Prandtl numbers the flow organized into CTCs. These columns are approximately axisymmetric, weakly interacting, and nearly steady. The authors showed that the steady-state mean temperature profile in the fully nonlinear regime is accurately predicted by the equations for planform convection. However, the planform approach cannot describe the individual CTCs seen in the simulation (Fig. 1). We present here a nonlinear, analytical model of an individual CTC which can be used as the basis of an atomistic description of the balanced equations composed of an ensemble of weakly interacting columns.

We use a search algorithm on the data set provided in [12] for $\tilde{\text{Ra}} = 40$, $\sigma = 7$ to identify well-formed and well-separated CTCs. These are azimuthally averaged to obtain axisymmetric profiles of the fields as a function of the radial distance r from the core and the height z within the CTC. The resulting profiles cluster around a well-defined mean; we use this mean as a fiducial CTC whose properties we model below. The details of the search algorithm and averaging protocol will be reported elsewhere.

For the model we assume that nonlinear horizontal interactions between columns are weak, in the sense that such interactions do not substantially affect their structure, while allowing passive advection of one column by another, i.e., we assume that the column structure is time-independent, axisymmetric, and identical to the fiducial CTC constructed from the data set. For such a CTC the nonlinear horizontal self-interaction vanishes identically. The net heat flux through the layer is described by the term $\overline{w\theta} = \overline{\theta \nabla_{\perp}^2 \phi}$ in Eq. (4). This includes contributions from CTCs as well as extra-columnar turbulence: $\overline{w\theta} = (\overline{w\theta})_{\text{CTC}} + (\overline{w\theta})_t$ where the latter term is the turbulent heat flux. Although not the main focus of this research, a simple model of the turbulent heat flux which allows one to gauge its impact on the columns and on the net heat flux is $(\overline{w\theta})_t = -\sigma^{-1} f_t(z) \partial_z \bar{T}$ where f_t is a shape parameter. We model the contribution from the columns as $c_f \langle w\theta \rangle$, where $\langle \cdot \rangle$ now denotes the horizontal integral over a single column, and the heat flux carried by a single column is multiplied by the number of columns per unit area c_f . Taken

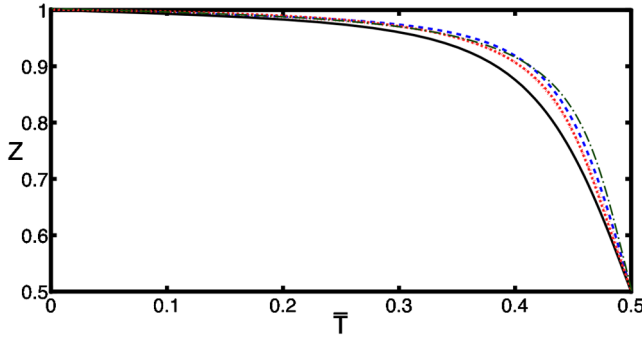


FIG. 2 (color online). Vertical profiles of the mean temperature \bar{T} in the upper half of the layer from the DNS [12] (solid line), Hankel with $f_t = 0$ (dashed line), Hankel with $f_t(z) = C \sin^2(\pi z)$ and $C = 115$ chosen such that $\text{Nu} = 15.53$ (dash-dotted line), and Bessel with $f_t = 0$ (dotted line) solutions at $\tilde{\text{Ra}} = 40$. The mean temperature is symmetric about $z = \bar{T} = 1/2$. The Hankel solutions use $k = 1.34 \exp\{0.153i\}$ when $f_t = 0$ and $k = 1.38 \exp\{0.153i\}$ when $f_t \neq 0$.

collectively, these assumptions imply that a single column satisfies

$$-\partial_z \phi = \omega, \quad (5)$$

$$\partial_z \psi = \sigma^{-1} \tilde{\text{Ra}} \theta + \nabla_r^4 \phi, \quad (6)$$

$$\phi \partial_z \bar{T} = \sigma^{-1} \theta, \quad (7)$$

$$\partial_z (c_f \langle \theta \nabla_r^2 \phi \rangle - \sigma^{-1} f_t \partial_z \bar{T}) = \sigma^{-1} \partial_{zz} \bar{T}. \quad (8)$$

Equation (8) may be integrated exactly in z , and its dependence on θ may be removed by the use of Eq. (7). Furthermore, integration by parts in the flux term $\langle \phi \nabla_r^2 \phi \rangle$ and the introduction of the Nusselt number (Nu), a nondimensional measure of the efficiency of heat transport defined by $\text{Nu} = -\partial_z \bar{T}|_0$, allows additional simplification of Eq. (8). With Eqs. (5)–(7) condensed down to a single equation for ϕ , the single column equations are

$$\partial_z^2 \phi + \nabla_r^2 (\tilde{\text{Ra}} \partial_z \bar{T} + \nabla_r^4) \phi = 0, \quad (9)$$

$$\partial_z \bar{T} = -\frac{\text{Nu}}{1 + f_t + c_f \sigma^2 \langle (\partial_r \phi)^2 \rangle}. \quad (10)$$

These equations, subject to impenetrable boundary conditions $\phi = 0$, $\bar{T} = 1$ at $z = 0$ and $\phi = \bar{T} = 0$ at $z = 1$ constitute our CTC model.

The simplest solution of the CTC model is separable and has a radial structure given by a Bessel function of the first kind: $\phi(z, r) = \hat{\phi}(z) J_0(kr)$. Since this solution has infinite heat flux and circulation, the solution is meaningful only in the presence of a finite cutoff r_0 . Choosing r_0 to satisfy $J_0(kr_0) = 0$ and defining $c_0 = c_f \langle J_0(kr)^2 \rangle_{r_0}$, the column equations become

$$[\partial_z^2 - k^2 (\tilde{\text{Ra}} \partial_z \bar{T} + k^4)] \hat{\phi} = 0, \quad (11)$$

$$\partial_z \bar{T} = -\frac{\text{Nu}}{1 + f_t + c_0 \sigma^2 k^2 \hat{\phi}^2}. \quad (12)$$

Given $\tilde{\text{Ra}}$ and k this is an eigenvalue problem for Nu . This type of problem arises in single-mode planform convection [15,24,25], and we do not reproduce its properties here. For the purposes of comparison of the predictions of Eqs. (11) and (12) with the simulations and the model proposed below, we use the critical value of k at the onset of linear instability as the scaled Rayleigh number increases, namely, $k_c = \pi^{1/3} 2^{-1/6} \approx 1.3048$ [dimensionally, $k_c^* = k_c (h\text{Ro})^{-1}$, where h is the layer depth], and use c_0 (equivalently r_0) as a fitting parameter. When $f_t = 0$ the best fit to $w(r, z = 1/2)$ for the fiducial CTC is obtained for $c_0 = 0.05$; since $c_f = 0.003$ [12] this value corresponds to $r_0 = 11.44$. This distance is less than half the typical intercolumn separation.

The resulting J_0 Bessel columns show reasonable accuracy in predicting the mean temperature (Fig. 2) and the vertical structure of the velocity, vorticity, and temperature perturbations (Fig. 3, insets), but fail to match the radial profile of CTCs seen in the simulations (Fig. 3). Moreover, the radial profiles of all the dependent variables are identical and depth independent, also in conflict with the simulations. Finally, the associated azimuthal velocity around a Bessel column decreases only as $r^{-1/2}$, and this slow decay results in strong interactions between columns which are inconsistent with visualization [12] of the numerical solutions.

We improve upon the J_0 Bessel solution by considering more general solutions of the column equations (9) and (10). We suppose that the radial structure is described by Hankel functions of the first kind, $H_0(kr) \equiv J_0(kr) + iY_0(kr)$, where Y_0 is a Bessel function of the second kind and $k \equiv |k| \exp\{i\alpha\}$ is complex, and write $\phi(z, r) = (\pi/8\sigma^2 c_f)^{1/2} H_0(kr) \tilde{\phi}(z) + \text{c.c.}$, where $\tilde{\phi} \equiv \tilde{\phi}_r + i\tilde{\phi}_i$. Since

$$\langle H_0(kr)^2 \rangle = \frac{4}{\pi k^2}, \quad \langle |H_0(kr)|^2 \rangle = \frac{4(\pi - 2\alpha)}{\pi |k|^2 \sin(2\alpha)}, \quad (13)$$

$\tilde{\phi}$ now solves the complex eigenvalue problem

$$[\partial_z^2 - k^2 (\tilde{\text{Ra}} \partial_z \bar{T} + k^4)] \tilde{\phi} = 0, \quad (14)$$

$$\partial_z \bar{T} = -\frac{\text{Nu}}{1 + f_t + (\pi - 2\alpha) \cot(2\alpha) |\tilde{\phi}|^2 + \tilde{\phi}_r^2 - \tilde{\phi}_i^2}, \quad (15)$$

subject to the boundary conditions $\tilde{\phi} = 0$, $\bar{T} = 1$ at $z = 0$, and $\tilde{\phi} = \bar{T} = 0$ at $z = 1$. This problem has two eigenvalues, and we solve it for the eigenvalues Nu and $|k|$ for $\tilde{\text{Ra}} = 40$ and different values of α . The latter are restricted to lie in the interval $0 < \alpha < \pi/12$ by the requirement that the solution decays away from the center and that no solution exists at $\tilde{\text{Ra}} = 0$.

The eigenvalue problem (14) and (15) is solved using a shooting method and the results confirmed using the Newton-Raphson-Kantorovich algorithm. The eigenvalues $|k|$ and Nu are relatively insensitive to the choice of α , and we select α to fit $w(r, z = 1/2)$ for the fiducial CTC

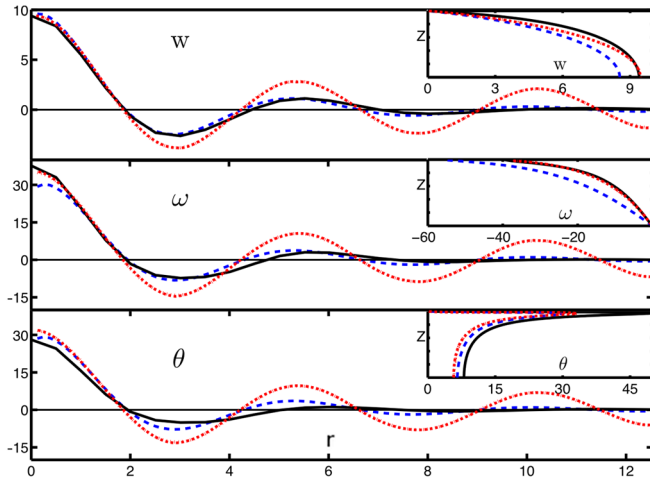


FIG. 3 (color online). Radial and vertical (inset) profiles of w , ω , and θ for the fiducial CTC from DNS [12] (solid line), and for the Hankel (dashed line) and Bessel (dotted line) columns with $f_t = 0$, showing $w(z = 1/2, r)$, $\omega(z = 1/96, r)$, $\theta(z = 1/96, r)$; these values were chosen to be near local maxima of the vertical profiles. The Hankel column fit uses $k = 1.34 \exp\{0.153i\}$. The vertical profiles are shown at $r = 0$ except for the Hankel solution for which we show $|\hat{\phi}(z)|$ since the amplitude at $r = 0$ is unbounded; the logarithmic singularity is present, but nearly invisible.

constructed from the data set. Figure 3 shows that the resulting Hankel fit matches simultaneously both the vertical and radial profiles of the fiducial CTC, apart from an integrable logarithmic singularity at the center of the column. The quality of the fit is robust: for the range of acceptable α the value of $|k|$ varies by less than 5%, and the radial structure of the solution varies relatively little.

In contrast to the Bessel solution the Hankel solution reproduces the z dependence of the radial profiles, although it overpredicts the heat flux through the layer. In particular, $Nu = 21.26$ at $\tilde{Ra} = 40$ instead of the DNS result $Nu = 15.53$. This discrepancy is the result of a nonlinear competition between the columns and extra-columnar turbulence, and can be eliminated by the inclusion of f_t (Fig. 2, dash-dotted line). For comparison the Bessel fit with $k = k_c$, $r_0 = 11.44$, and $f_t = 0$ yields $Nu = 19.18$. However, the heat flux parametrization does not account for enhanced lateral mixing by vortex interactions among columns and turbulent plumes [10,12], and duly overpredicts the degree of isothermality of the interior relative to the DNS result (Fig. 2).

The Hankel solutions of the column equations are currently the best model of CTCs, displaying a significant improvement over linear [21] and nonlinear CTC models based on Bessel functions. Consequently, the single column Hankel solutions provide the best possibility for understanding CTC interactions (pairwise and ensemble) as well as showing potential for parametrizing convective mixing within large scale ocean circulation models. These

solutions, moreover, constitute a significant improvement over other models of coherent structures in geophysical flows, such as hetons [26], which are a hydrostatic, two-layer model of an essentially nonhydrostatic, continuously stratified process.

This work was supported by NSF FRG Grants No. DMS-0855010 and No. DMS-0854841. The authors would like to thank Geoff Vasil, Harvey Segur, Michael Sprague, and an anonymous referee for helpful comments.

- [1] M. Miesch, *Sol. Phys.* **192**, 59 (2000).
- [2] M. Evonuk and G. A. Glatzmaier, *Planet. Space Sci.* **55**, 407 (2007).
- [3] J. Marshall and F. Schott, *Rev. Geophys.* **37**, 1 (1999).
- [4] M. DiBattista and A. Majda, *Proc. Natl. Acad. Sci. U.S.A.* **96**, 6009 (1999).
- [5] G. F. Carnevale, J. C. McWilliams, Y. Pomeau, J. B. Weiss, and W. R. Young, *Phys. Fluids A* **4**, 1314 (1992).
- [6] D. I. Pullin and P. G. Saffman, *Annu. Rev. Fluid Mech.* **30**, 31 (1998).
- [7] S. Sakai, *J. Fluid Mech.* **333**, 85 (1997).
- [8] P. Vorobieff and R. Ecke, *J. Fluid Mech.* **458**, 191 (2002).
- [9] B. M. Boubnov and G. S. Golitsyn, *J. Fluid Mech.* **167**, 503 (1986).
- [10] K. Julien, S. Legg, J. McWilliams, and J. Werne, *J. Fluid Mech.* **322**, 243 (1996).
- [11] R. P. J. Kunnen, H. J. H. Clercx, and B. J. Geurts, *Phys. Rev. E* **74**, 056306 (2006).
- [12] M. Sprague, K. Julien, E. Knobloch, and J. Werne, *J. Fluid Mech.* **551**, 141 (2006).
- [13] S. Chandrasekhar, *Hydrodynamic and Hydromagnetic Stability* (Oxford University Press, Oxford, England, 1961).
- [14] E. Knobloch, in *Lectures on Solar and Planetary Dynamos* (Cambridge University Press, Cambridge, England, 1994).
- [15] K. Julien and E. Knobloch, *Phys. Fluids* **11**, 1469 (1999).
- [16] E. King, S. Stellmach, J. Noir, U. Hansen, and J. Aurnou, *Nature (London)* **457**, 301 (2009).
- [17] K. Julien, S. Legg, J. McWilliams, and J. Werne, *J. Fluid Mech.* **391**, 151 (1999).
- [18] K. Julien and E. Knobloch, *J. Fluid Mech.* **360**, 141 (1998).
- [19] G. Taylor, *Phil. Trans. R. Soc. A* **223**, 289 (1923).
- [20] J. Proudman, *Proc. R. Soc. A* **92**, 408 (1916).
- [21] J. W. Portegies, R. P. J. Kunnen, G. J. F. van Heijst, and J. Molenaar, *Phys. Fluids* **20**, 066602 (2008).
- [22] H. P. Greenspan, *The Theory of Rotating Fluids* (Cambridge University Press, Cambridge, England, 1968).
- [23] K. Julien, E. Knobloch, R. Milliff, and J. Werne, *J. Fluid Mech.* **555**, 233 (2006).
- [24] A. Bassom and K. Zhang, *Geophys. Astrophys. Fluid Dyn.* **76**, 223 (1994).
- [25] K. Julien and E. Knobloch, *J. Math. Phys. (N.Y.)* **48**, 065405 (2007).
- [26] S. Legg and J. Marshall, *J. Phys. Oceanogr.* **23**, 1040 (1993).
- [27] J. Clyne, P. Mininni, A. Norton, and M. Rast, *New J. Phys.* **9**, 301 (2007).